

Effects of Long-Term Dynamic Loading and Fluctuating Water Table on Helical Anchor Performance for Small Wind Tower Foundations

Amy B. Cerato, P.E., A.M.ASCE¹; and Rory Victor, A.M.ASCE²

Abstract: The application of this study is to use helical anchors as a foundation system for small wind tower (1–10 kW) guyed cables. Helical anchors are currently used to anchor guyed cables of cell or transmission towers. However, the increased dynamic vibrations a wind turbine adds to the tower and foundation system under working loads, as well as extreme environmental conditions (e.g., straight line winds, ice load, or sudden furling shocks), require additional knowledge about the behavior of helical anchors. These field conditions were simulated in this study from tower-instrumented field data on wind speed and tower response. These tower responses were then transmitted to the helical anchors through an extensive, large-scale testing program that included monitoring the performance of the helical anchor foundation under dynamic loads, subject to natural variations in both wind regimes, precipitation (water level) and variations in helical anchor geometry. This paper compares the uplift prediction methods used in helical anchor design as well as discusses the effects of long-term dynamic loading and fluctuating water table on helical anchor performance.

DOI: 10.1061/(ASCE)CF.1943-5509.0000013

CE Database subject headings: Anchors; Dynamic loads; Creep; Uplifting; Water table; Towers; Geometry.

Introduction

Foundation systems designed for pullout or tensile loads are classified as anchors. These foundation types are used to protect structures against overturning or pullout forces, but do have the capability to resist compressive, lateral, and other loading combinations. Electrical transmission towers, retaining walls, offshore and hydraulic structures, and many domestic structures are subjected to loads (e.g., earthquake, wind, lateral earth pressure, waves, and hydrostatic pressure) that generate strong tensile forces that overturn or pullout such structures. Anchors are created in a variety of configurations ranging from plate anchors, pile anchors, grouted anchors, prestressed concrete anchors, and single and multiple-screw helical anchors. Helical anchors are fabricated by welding single or multiple helical plates to a steel rod at predetermined spacing. Helical anchors are installed into the ground by applying torque to the shaft, causing the anchor to screw through the soil. An axial compression force is applied to ensure that the anchor advances through the soil.

The main advantages of helical anchors compared to conventional concrete-cast anchors include: their relative ease for installation depending on soil conditions, mobility, cost-effectiveness, and providing overturning and uplift stability immediately after

installation due to the elimination of the curing that is encountered in concrete anchors. Many factors are involved in predicting helical pullout capacities, ranging from site conditions (i.e., water table location, active zone location, frost level, etc.), anchor geometry, subsurface stratigraphy, and soil strength parameters (i.e., cohesion, friction angle, unit weights, etc.).

The performance of a helical anchor for use as a wind tower guyed cable foundation, however, not only encompasses the uplift capacity, but also the creep (magnitude and rate). Creep is anchor movement under load, over time. When environmental conditions change (e.g., rising water table) after anchor installation, the effective stress above the helices decreases and therefore the soil strength decreases, creating a tendency for anchors to creep. When the water recedes, and/or the tension is removed from the cable (wind direction shift), the anchor may return to its original installed position due to soil elastic deformation or soil disturbance caused during installation and subsequent dynamic loading. The slack in the cable would then have to be removed to avoid a potential large movement in the tower the next time the wind shifted, which would put the turbine at risk. Apart from environmental changes, creep can occur if the loads are large enough to overcome the soil resistance. Excessive, continuous creep in wind tower foundations is not desirable. This study was launched in order to provide the small wind power industry with field-scale tests subjected to realistic loads showing that helical anchors are a viable foundation alternative for wind power in remote locations where concrete is not an option.

Methods to Determine Uplift Capacity

The two most common methods used to predict the uplift capacity of multi-helix anchors are the cylindrical shear and the individual bearing methods (analytical methods based on soil properties). These two methods require detailed prior knowledge of soil prop-

¹Assistant Professor, Dept. of Civil Engineering and Environmental Science, Univ. of Oklahoma, 202 W. Boyd St., Room 334, Norman, OK 73019 (corresponding author). E-mail: acerato@ou.edu

²Construction Engineer, Exxon-Mobil Development Company (EMDC), 17001 North Chase Dr., Houston, TX 77060; E-mail: roryv@ou.edu

Note. This manuscript was submitted on July 8, 2008; approved on December 10, 2008; published online on March 11, 2009. Discussion period open until January 1, 2010; separate discussions must be submitted for individual papers. This paper is part of the *Journal of Performance of Constructed Facilities*, Vol. 23, No. 4, August 1, 2009. ©ASCE, ISSN 0887-3828/2009/4-251-261/\$25.00.

erties. Usually a combination of in situ testing (i.e., CPT, DMT, BST, etc.) and laboratory testing (i.e., triaxial, unconfined compression, direct shear, etc.) is needed to predict the uplift capacity, which can be time consuming and expensive. Even with some prior knowledge of soil properties, site conditions may be highly variable and one soil boring within the tower construction site may not capture all of the subsurface heterogeneity. For uplift capacity in sand, the friction angle and uplift coefficient of lateral earth pressure are needed. However, for clay, the required parameters are undrained shear strength and adhesion (Mitsch and Clemence 1985; Mooney et al. 1985).

A less intensive empirical method that relates the installation torque to a predicted load capacity in both tension and compression could supply a “quick and clean” method to predict uplift capacity of helical anchors. Hoyt and Clemence (1989) analyzed 91 uplift load test at 24 different sites within various soil types (i.e., sand, silt, and clay soils) in short term loading conditions. Their findings demonstrated that the consistency of the torque correlation modeling fared better when compared to the load capacity models of cylindrical shear and individual bearing. This is probably due to the fact that torque is taken at every anchor location, but the theoretical analytical models rely on location specific data (bore holes), of which there are fewer. The proposed formula from Hoyt and Clemence relates the ultimate uplift capacity of the helical anchor to its installation torque

$$Q_{ult} = K_t \times T \quad (1)$$

where Q_{ult} =ultimate uplift capacity [kN (lb)]; K_t =empirical torque factor [$m^{-1}(ft^{-1})$]; and, T =average installation torque [kN-m (lb-ft)].

K_t values vary according to shape of anchor shaft, diameter of shafts, soil conditions, and other properties; a default K_t value of $33 m^{-1}$ ($10 ft^{-1}$) for Type SS (square shaft) conditions is recommended. Installation resistance does give insight into soil properties and uplift capacity the soil may yield with a particular anchor geometry, but it does not incorporate the effects that dynamic loads (i.e., operational loads and wind loads) and fluctuating water tables will have on capacity in the future.

The default value used in tension, $K_t=33 m^{-1}$ ($10 ft^{-1}$), was significantly less (i.e., 16 to 33 percent less) than values that were actually calculated after the compression test capacities were observed. This difference can be attributed to the fact that the lead helix rests on a relatively undisturbed soil stratum in compression applications, but in tension the trailing helix bears on the soil affected by the installation of both the lead and trailing helices (Hargrave and Thorsten 1992). Torque measurements taken during installation indicate soil strength (Perko 2000). However, the torque versus capacity relationship may not be valid where the lead plate encounters hard material, which is known as refusal condition. Most manufacturers agree that torque/uplift capacity correlations are not valid where the top helix is less than 5 diameters below the surface (Pack 2000). The torque correlation method was developed empirically, and even though it is widely used, it lacks explicit definition in geotechnical concepts.

Hoyt and Clemence (1989) concluded that all three methods, cylindrical shear, individual bearing, and torque correlation, exhibit overpredictions and a factor of safety should be used. The torque correlation method yielded more consistent results for uplift capacity, which may be due to the elimination of several variables including soil test data, spatial variation in the soil properties between anchor and soil boring locations, or changes in soil properties over a testing period that play a major factor in the

cylindrical and individual bearing method. Hoyt and Clemence (1989) suggest that the torque correlation be used as boundary check for the other two methods.

Dynamic Loading Effects on Uplift Capacity

Interest in the dynamic capacity of helical anchors has increased over the past decade due to some of the offshore applications of helical anchors. However, this interest has not led to many studies that discuss the effects of helical anchors that are subjected to dynamic loads (i.e., ocean waves, wind loads, and etc.). Previous research on piles (Hanna et al. 1978; Clemence and Smithling 1984; Trofimenkov and Mariupolskii 1965; Dejong et al. 2003; Dejong et al. 2006) has shown that cyclic loading has a degrading effect on the strength of both cohesionless and cohesive soil and thereby, pile/anchor behavior; however, some repeated load applications (cyclical loading) tend to increase the post-dynamic static capacity of a pile/anchor by stiffening the soil-anchor system. Total upward anchor movement is noticed to decrease when anchor is under static pressure loadings (Clemence and Smithling 1984). Depending on anchor depth and sand characteristics, Ghaly and Clemence (1999) in closure discussions, reports that the upward creep for one cycle is almost 100% recoverable if [cyclic loading (P_c)/ the ultimate static (P_{ud}) capacity] ratio is under 25%. With the increase in P_c/P_{ud} and/or the number of cycles, the percentage of cyclic creep recovery decreases and the post static capacity is suggested to decrease as well (Hovland 1993). Increasing step loads in uplift decrease the ultimate resistance 10–20 percent, independent of the soil (Trofimenkov and Mariupolskii 1965).

Hanna and Al-Mosawe (1981) noticed that prestressing an anchor can increase the life of an anchor significantly by reducing the rate of displacement under loading. An unproven belief is that prestressing techniques automatically allows for the effects of repeated loadings. In experiments by Hanna and Al-Mosawe (1981), it was demonstrated that a more severe loading system was 0–60% instead of 30–80% of the ultimate static load (P_u) due to the loss of prestressing (30% of P_u) over a span ranging from 0–60% of the P_u . Under repeated loading conditions, the higher the loading changes the faster failure was approached (Hanna et al. 1978). A repeated loading does have a gradual effect on an anchor by reducing its prestressing over a period of time, in which it reverts back to the behavior of a dead anchor (Hanna and Al-Mosawe 1981). The higher the prestress value the greater the life of the anchor provided that the applied repeated loads are less than the prestress values (Hanna and Al-Mosawe 1981).

Andreadis et al. (1981) concluded that the basic mode of response is essentially unchanged for different sizes of anchors, but the size differences display significant scale effects with the larger anchor displaying the weaker repeated loading behavior. The rate of soil flow around the anchor is largely dictated by the relative elastic displacement per loading cycle, which is great for the larger anchor system resulting in faster cyclic strength deterioration. Anchors subjected to sustained-repeated loading are subjected to increased displacements at the start of testing due to higher imposed peaks and larger cavities created, but as the test progresses the system appeared to become more stable, although displacement never completely ceases. If cyclic loading amplitudes exceed a critical value (i.e., ultimate static uplift capacity), the net upward displacement for successive load repetitions increases and the system fails (Andreadis et al. 1981).

Table 1. Subsurface Properties

Depth (m)	Layer number	PL	LL	PI	Activity	Specific gravity	USCS symbol	Average blow count from SPT	Friction angle/undrained shear strength	Group name
0–0.91	1	20.0	49.0	29.0	0.9	2.7	CL	7	57.9 kPa	Lean clay with sand
0.91–2.1	2	17.0	33.3	16.3	0.7	2.7	CL	15	89.7 kPa	Sandy lean clay
2.1–4.6	3	NP	NP	NP	NP	2.7	SM	8	35°	Poorly graded sand
4.6–6.7	4	20.0	26.0	6.0	0.4	2.7	CL-ML	3	17.9 kPa	Silty clay with sand
6.7–7.6	5	NP	NP	NP	NP	—	—	50/.45	—	Weathered shale

Prasad and Rao (1994) conducted three phase laboratory tests on model (regular piles) and helical piles in marine clay (three phase=lateral static load tests, lateral cyclic load tests, and vertical pullout tests), it was concluded that lateral cyclic loading affects the pullout capacity of piles (no plates) substantially, while helical anchor uplift capacities, under similar conditions, experience very little influence from the three phase testing regime. At lower (i.e., 30%) lateral loading levels (lateral cyclic load/static lateral capacity), model pile pullout capacities are still stabilized with pile deflections less than 3% of pile diameter, however, at lateral load levels of 50–70% (high levels) reductions were experienced as deflections increased beyond 3% up to 10% of pile diameter. Prasad and Rao (1994) concluded possible reasons for model pile lateral and pullout capacity reductions under lateral cyclic loading is the formation of a gap around the pile and loss in strength within the soil mass. In the case of helical piles that had as high as 10% of shaft diameter deflection there was no reduction. In helical piles at depth ratios of $H/D=0$ and $H/D=2.5$, the gap formation and loss in strength during cyclic loading are confined to a narrow zone of the soil adjacent to pile shaft, thereby causing no uplift capacity reductions. In $H/D=4$ conditions, there is marginal reduction in uplift capacity due to the gap and loss of soil strength in that narrow zone, because this reduces the shaft adhesion resistance which has marginal strength when the top helix is at such deep depths (Prasad and Rao 1994).

Testing Site

The testing site was located directly east of the University of Oklahoma, Norman Campus Fears Structural Engineering Lab. Anchors were installed about 4.6 m (15 ft) on-center to eliminate any possibility of soil interaction between adjacent anchors. The typical default minimum spacing between adjacent anchors is 5D of the largest helix, but not less than 1.5 m (5 ft). The soil profile of the site was determined using several hand auger borings, existing soil maps, and previous explorations of the site. Table 1 presents a summary of the soil properties which are displayed as a generalized cross section in Fig. 1. It should be noted that the subsurface was more variable than what is shown here based in the torque readings at each anchor location, however it was difficult to display the pockets of soil that did not extend longitudinally and latitudinally throughout the profile.

Fig. 1 also shows the helical anchor locations in relationship to each other and the soil profile. The water table depth was taken from a previously installed well near the testing site. The average depth of the water table from March 16, 2007–March 24, 2008 was approximately 2.1 m (6.9 ft). The lowest and highest water table recorded at the site during the same time period was 4.48 m (14.7 ft) (March 16, 2007) and 0.61 m (2 ft) (July 16, 2007), respectively.

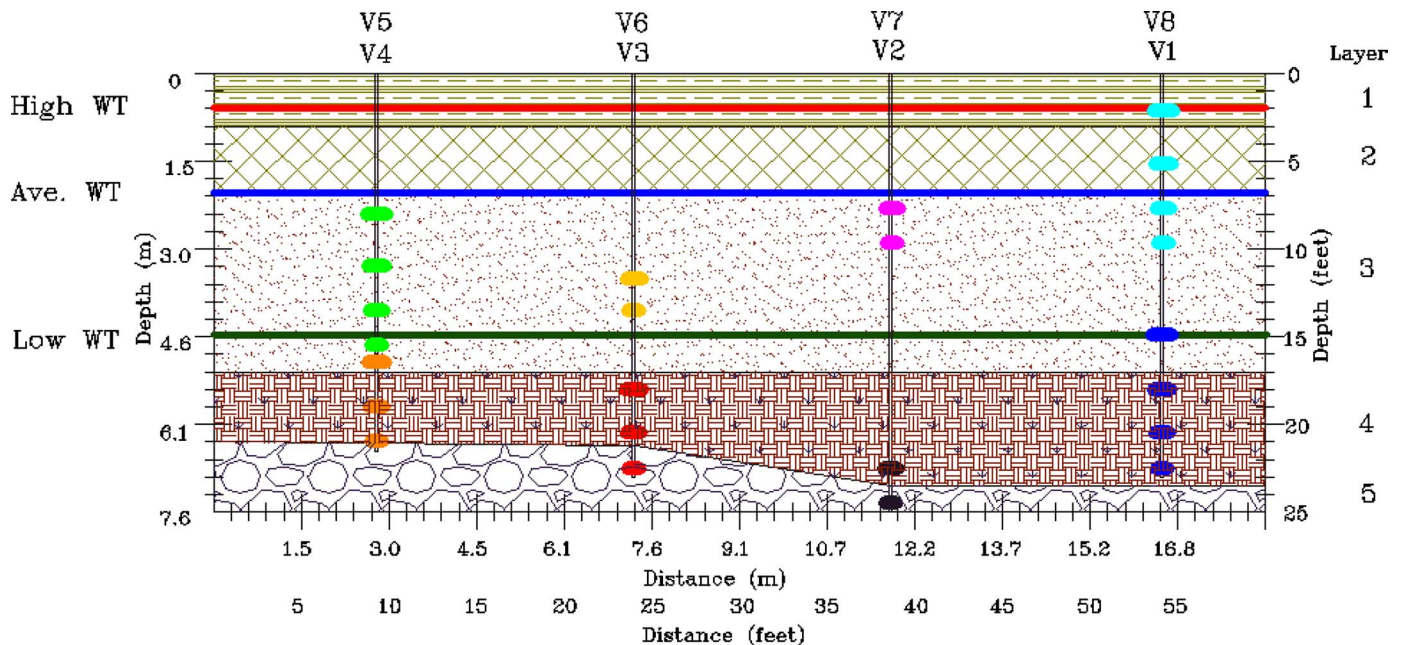


Fig. 1. Foundation soil cross section with installed anchors

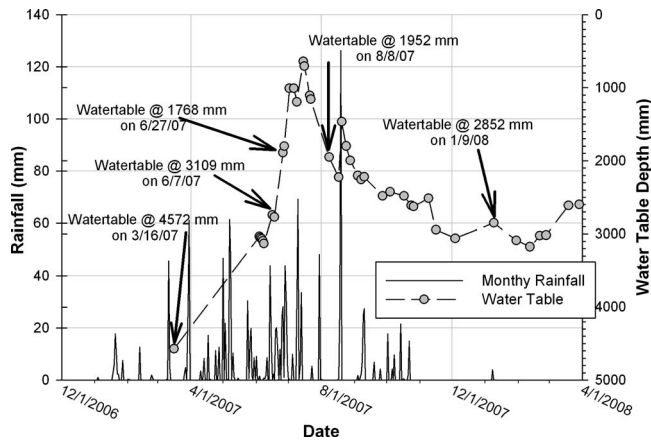


Fig. 2. Water table and rainfall monitoring

Groundwater Variation

The presence of water table in foundation soils is an important factor in foundation design, and the design of helical anchor systems are not an exception. Throughout the installation and testing procedures the water table and rainfall data were monitored to quantify the effects that a varying water table (i.e., rising water table) has on the uplift capacity of anchors in static and dynamic conditions. Fig. 2 gives an illustration of the rainfall data (compiled from Oklahoma Mesonet data) and the water table depth over the installation and testing periods of the anchors.

The results provide insight on how rainfall affects water table in this area. V1 and V2 were installed at the lowest recorded water table depth of 4.57 m (15 ft) on March 16, 2007. This water table had been relatively constant for the past 20 years. However, while testing was ongoing, a record rainfall amount fell over 21 days in a row in June and July, which caused the water table to rise to a record high of 0.61 m (2 ft) below the ground surface. During these record rainfall events, V1 and V2 were statically tested on June 6 and June 27, respectively. The results were less than desirable as will be discussed in more detail later in the paper, and therefore, on August 8, 2007, after the water table receded about 1.37 m (4.5 ft) from its maximum level, the anchors were uninstalled and reinstalled to obtain a new torque profile with all installation criteria met, now understanding the range of water table fluctuations. A small peak in the groundwater table was observed around August 18, 2007, after a large rainfall event, which was followed by a water table drop to levels ranging from 2.59–3.0 m (8.5–10 ft) near the completion of all tests.

Anchor Installation

Two anchors were installed on March 16, 2007 with the water table at 4.57 m (15 ft) below the ground surface. Six anchors were installed on August 8, 2007 when the water table was at 2.0 m (6.7 ft) below the ground surface. Each anchor was screwed into the earth with a high-torque hydraulic torque motor which was mounted on a, Bobcat®, skid steer loader equipped with an in-line torque-monitoring device.

The helical anchors installed were 4.44 cm (1.75 in.) square shaft anchors supplied by Hubbell Power Systems/Chance (Missouri). The torque rating for this particular series of helical anchors is 14.9 kN-m (11,000 ft-lb) and the ultimate tension capacity limit (using the $Q=K_r T$ with $K_r=33 \text{ m}^{-1}$ or 10 ft^{-1}) is

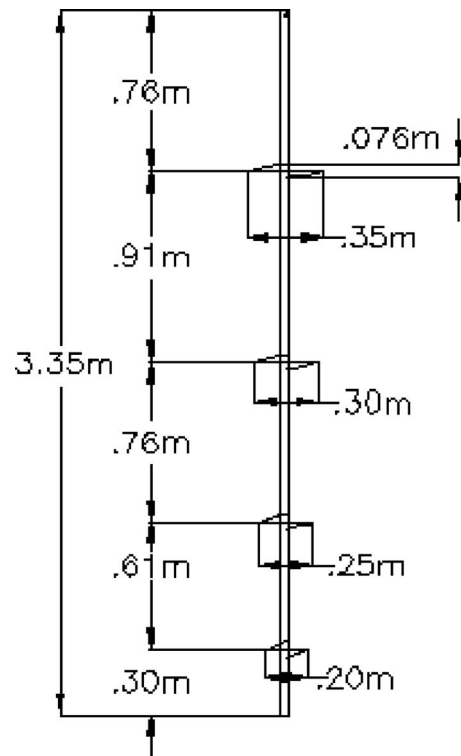


Fig. 3. 4-helix helical anchor geometry

489.5 kN (110 kip). However, the ultimate mechanical tensile strength is limited by the coupling to 444.5 kN (100 kip). Fig. 3 displays the 4-helix anchor plate spacing and plate diameters installed. The helical plate spacing and diameters decrease from top to bottom and the pitch remains constant at each plate. The 3- and 2-helix configurations are identical to the 4-helix, by just removing the top 1 and top 2 helices, respectively.

Each anchor (except V1) was installed to a depth that met the two-part criteria: (1) the top helix had to be embedded at least 5D (D=diameter of top helix) into the subsurface; and/or (2) the average torque in the final 1 m (3 ft) of installation must meet or exceed the designated torque value for the small wind tower application (4.3 kN-m or 3,200 ft-lb). This design torque value was determined based on the maximum design load for a 33.3 m (100 ft) wind tower with a 10 kW turbine. The towers are designed to withstand 128.8 km/h (80 mi/h), Exposure D winds [gusts > 193.2 km/h (120 MPH)]. The maximum design load was 71.3 kN (16,000 lb) and therefore, to create a factor of safety of 2, this load was doubled to determine the target installation torque for the anchors. Fig. 4 shows the installation torque values with depth and Table 2 summarizes the final depth of installation, average final torque, depth to top helix and embedment (H/D or depth of top plate/diameter of top plate) ratios. The average final torque signifies the mean value of the last three torque measurements. The reason that Anchor V1 was not installed to a depth to meet the “5D” requirement was that it achieved a very high torque within the first 10 ft, and the goal of the project was to try and keep all anchors with a certain range of installation torque values to be able to study performance. However, it was not anticipated that the water table would rise 3.9 m (13 ft), drastically reducing this anchors predicted capacity. It is extremely important to have a good understanding of high water table levels when installing anchors and ensure that the top helix is always below the water table to provide an adequate foundation. This should be

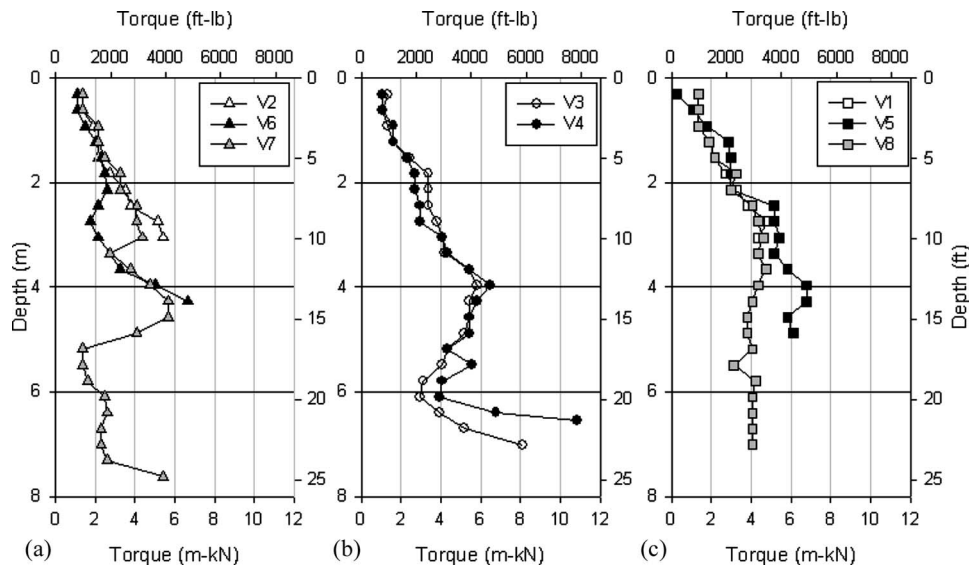


Fig. 4. Installation torque plot: (a) 2-helix; (b) 3-helix; and (c) 4-helix

a third criterion for the design of helical anchors used in tension applications.

Installing anchors to the same depth was preferable for a more direct performance comparison, however, as can be seen in Fig. 1, paired anchors were not installed to the same depth, within the same soil layer. The reason for this is that the subsurface was variable enough across the site that target torque values were not achieved at the same depths, even with anchors of the same geometry. Limitations in capacity were met in the field with Anchors V3, V7, and V8. Due to a weak pocket in the subsurface, these three anchors could not meet the target torque of 4.3 m-kN (3,200 ft-lb). Anchors V3, V4, and V7 encountered a hard/dense layer during installation, which is known as the refusal condition. The significant increase in torque at the final depth was probably caused by the 0.2 m (8 ft) helix penetrating into the weathered shale. This helix penetration was minimal, however, at 0.1–0.15 m (4–6 ft), and the recommended minimum depth of penetration into a bearing layer to use for design is 3D. Therefore, the final torque values of Anchors V3, V4, and V7 were discarded, and the three previous torques were used to calculate the effective average installation torque.

Dynamic Testing

Five anchors (V3, V4, V5, V6, and V8) were dynamically loaded for 2–4 weeks, followed by a postdynamic static test. V7 was only statically tested to have a comparison anchor to V6 to show the effects of dynamic loading on long-term uplift capacity. Anchors V1 and V2 were tested statically and will be used to show water table influence on anchor performance.

All tests used to determine the capacity of the anchors under tension load were completed with similar setups. The setup included a variable layer of cribbing, depending on the shaft height above the ground surface, which changed on a test to test basis. The cribbing consisted of layers of railroad ties stacked perpendicular at each layer. Two 5.5-m (18-ft) long W beams (reaction beams) were placed on the ties, with the shaft bisecting the reaction beams. A hydraulic jack/actuator was mounted on top of the reaction beam to test the anchors in tension. In dynamic testing, potentiometers/wire pots were the instruments used to measure the displacements. All instruments were mounted on a reference beam installed perpendicular to the reaction beams and not in

Table 2. Anchor Installation Information

Anchor symbol	Geometry	Average final torque [kN-m (lb-ft)]	Final depth [m (ft)]	Top helix depth [m (ft)]	H/D
V1	4-helix	4.6 (3,200)	3.05 (10)	0.76 (2.5)	1.7
V2	2-helix	5.3 (3,500)	3.05 (10)	2.29 (7.5)	9.0
V3	3-helix	4.0^a (2,970)	7.01 (23)	5.49 (18)	18.0
V4	3-helix	4.9 (3,633)	6.55 (21.5)	5.03 (16.5)	16.5
V5	4-helix	6.2 (4,600)	4.88 (16)	2.44 (8)	6.9
V6	2-helix	5.0 (3,666)	4.27 (14)	3.51 (11.5)	13.8
V7	2-helix	2.4^a (1,766)	7.62 (25)	6.86 (22.5)	27.0
V8	4-helix	4.1^a (3,000)	7.01 (23)	4.57 (15)	12.9

Note: Bold data are anchors that did not meet design average final torques.

^aDid not meet the design average final torque.

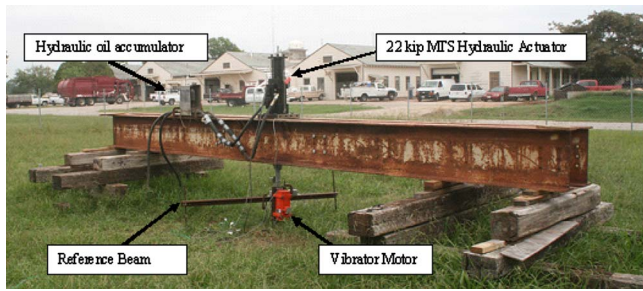


Fig. 5. Dynamic loading setup

contact with the foundation ground within a 1 m (3 ft) radius from the anchor shaft. Fig. 5 displays the basic setup for the dynamic test.

Seating loads were applied to the anchor ranging between 10–20% of its predicted ultimate static uplift capacity. Once the cribbing and anchor displacement was sustained at an equilibrium bearing pressure (minimal settlement), testing loads were applied.

All dynamic loads were applied in a sustained-repeated loading condition (Clemence and Smithling 1984). Testing procedures followed the sustained-repeated loading pattern, where the anchor remained in tension (8.9 kN or 2,000 lbs) throughout the entire testing period to simulate operating wind loads as experienced from a guyed wire anchor foundation. Previous investigations at Bergey Windpower (Norman, OK) estimated that guyed wires connected to wind towers were under constant tension of about 4.45 kN (1,000 lbs), with vibrations in the 3–5 hertz range depending on the wind intensity. Regular operating loads on the anchor during testing oscillated between 4.45–35.6 kN (1,000–8,000 lb). Extreme wind-shock loadings were applied in 0.5–2 hr intervals that simulated extreme operating and weather conditions (e.g., hurricanes, tornadoes, and high winds) with oscillating load patterns ranging from 4.45–88.9 kN (1,000–20,000 lb). This range of loading encompassed the capacity of the 9.50 kN (22,000 lb) actuator, and depending on individual anchor capacity, the upper load limit (88.99 kN or 20,000 lb) created a factor of safety (FS) condition ranging from 1.5 (V3) to 2.3 (V5) at the maximum loads applied. All dynamic data was recorded by data acquisition software at 50 hertz.

Dynamic Testing Results

Long-term, 2–4 wk, dynamic testing was completed on 5 anchors before the anchors were tested in static conditions. The dynamic (cyclic) testing regime was used to simulate operational conditions of a wind turbine tower and extreme weather conditions (i.e., tornadoes, wind gust, etc.). Fig. 6–8 summarize the dynamic test hourly over the testing period. They also indicate the maximum design load ($FS=2$) of the guyed cables. The cyclic loading was applied between 3–5 hertz in a sustained-repeated loading (anchor was always in tension of at least 4.45 kN or 1,000 lb) and data was acquired at a 50 hertz frequency. Sustained-repeated loading was an important principle in this research. Keeping the anchor from experiencing compression was imperative for maintaining safety on-site and preserving the cribbing configuration. Also, helical anchors used for guyed cable foundation would never experience compression loading. Because to the immense data sets, hourly summarization was used to adequately analyze the data.

A general behavior experienced by all anchors was the significant movement during the seating load, which cannot be solely explained by the slack in the couplings. Each coupling has a tolerance of approximately 0.16 cm (0.0625 in.). The movement of most anchors was about 1.3–2.5 cm (0.5–1 in.), when a seating loading was applied in a cyclic load arrangement from 8.9–17.8 kN (2,000–4,000 lb) or less. This seating movement may have been the result of excessive soil disturbance during installation, shaft alignment issues, etc. Since all guy tower cables are pre-loaded to 10% of the mean breaking cable strength, this seating movement can be overcome. Also, if the wind were to die down, or switch directions, the anchor could return to its original position (settling ~2.5 cm or 1 in.) unless soil filled in the cavities below the helices. It was seen in the displacement versus load results of both static unload-reload cycles and long term dynamic testing, that depending on the soil type, the soil would fall down around the helices, filling in the cavities and keep the anchor from returning to its original position. Other researchers [Hanna and Al-Mosawe 1981] have suggested that helical anchors should actually be prestressed to reduce the rate of displacement under loading.

Fig. 6 describes the behavior of Anchors V3 and V4 (both

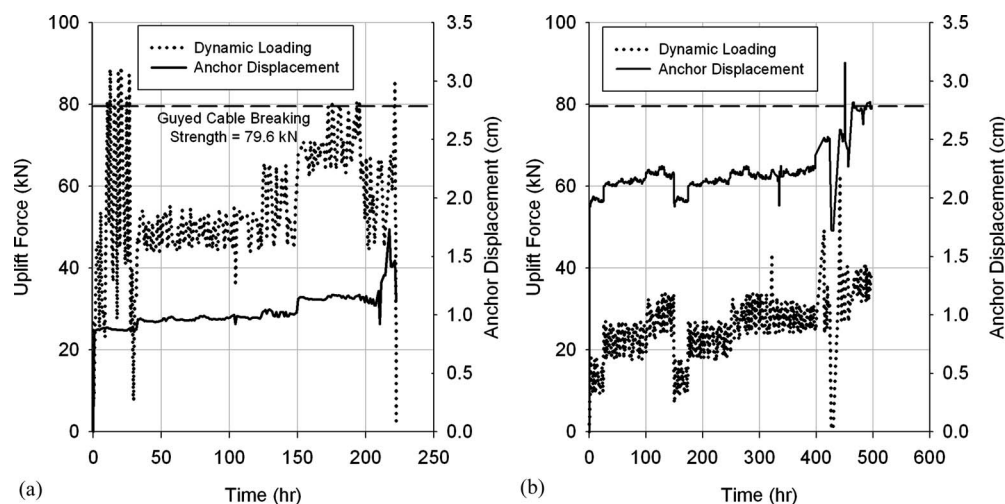


Fig. 6. 3-helix long-term dynamic test: (a) Anchor V3; (b) Anchor V4

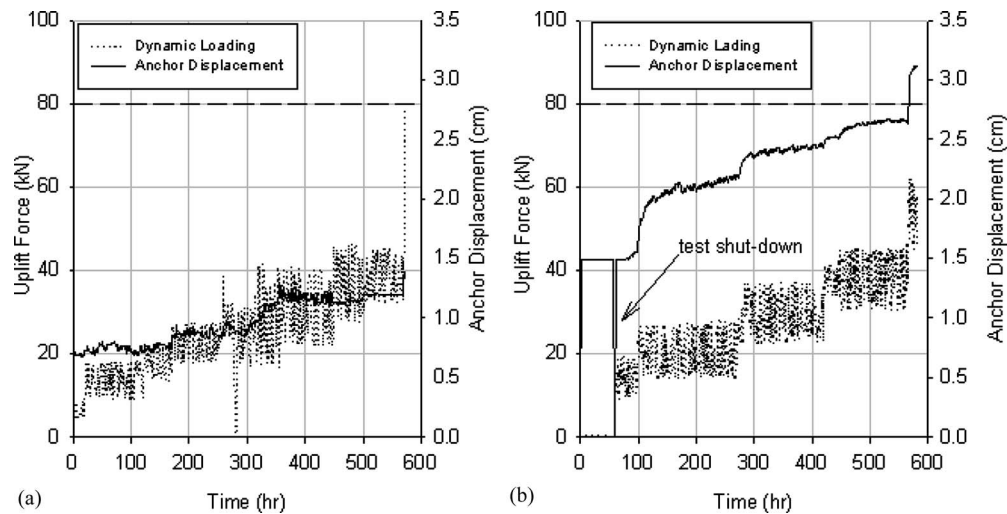


Fig. 7. 4-helix long-term dynamic test: (a) Anchor V5; (b) Anchor V8

3-helix anchors), tested from September 10–27, 2007 and September 27–October 13, 2007, respectively.

Anchor V3 had a predicted uplift capacity of 188.1 kN or 42,300 lb (torque correlation) and the anchor performed well in minimizing long term creep. As the results show, the 3-helix anchor performed satisfactorily in guyed cable applications (<79.8 kN or 17,900 lb) where the anchor remained relatively constant for that loading application. The anchor was also able to withstand substantial loads between 66.6 and 88.9 kN (15,000 and 20,000 lb) for long periods of time at the start and ending of testing. During both V3 and V4 tests, the water table remained relatively constant only receding about 25.4 cm (10 in.). In contrast to anchor V3, there was a large displacement for the same seating load (2 cm or 0.8 in.). However, for the remainder of the test, when subjected to loads between 9.81 and 58.9 kN (2,000 and 13,000 lb), the anchor moved only an additional 0.6 cm (0.2 in.). This anchor was subjected to much lower loads over a longer time span than V3, but it is predicted that V4 would have performed similarly to V3 under a similar loading regime because of their similar torque installations and similar environmental conditions at testing time.

Fig. 7 shows the dynamic test for both 4-helix anchors, V5 and V8, performed from October 18 through November 13, 2007 and February 27–March 21, 2008, respectively. The results indicate V5 resisted upward displacement (creep) very well and after a 0.75 cm (0.3 in.) initial displacement with a low seating load, showed minimal creep throughout the remainder of the test. The anchor experienced a spike in displacement only after the guyed cable design threshold was surpassed at the end of the test, however, performed remarkably well under such an intense shock load. Anchor V8 was predicted (torque correlation) to resist an ultimate uplift force of 133.5 kN (30,000 lb), which was well above the average applied loads resulting in a factor of safety of around 5 for the majority of the test and a factor of safety around 1.6 at the end of the test under the load of 88 kN. Pack (2000) recommended a factor of safety of 2 to minimize creep based on results showing creep of an anchor under sustained static loading, not continually increasing incremental dynamic loading. However, as the results show, even when the factor of safety was approximately 5, the anchor experienced considerable displacement during low seating loads. This seating load displacement was over half of the total displacement experienced throughout

the test. What can also be seen is the nearly 100% recovery of displacement when the load was removed. This shows that when the anchor was pulled with only a small seating load, the anchors moved a significant amount to find firm bearing material, and soil had not yet flowed around the helices filling in the void. It should be noted that significant movement during the seating load after installation of helical anchors is not often seen, however, the movement seen in this particular study could be because of a poor installation. There were large voids around each anchor shaft and some of the deeper anchors could have been slightly inclined, which caused the anchor to right itself vertically during the seating load and show larger movements than normal. After the displacement at the seating load, the anchor performed fairly well under normal cyclic loads, and only displaced an additional ~1 cm (0.4 in.), which compared well with anchor V5 [0.75 cm (0.3 in.) creep past the seating load displacement], under a similar loading program (magnitude and duration).

In Fig. 8 the dynamic uplift behavior of Anchor V6 is shown, which was tested November 30–December 19, 2007 (water table variation of about 12.7 cm or 5 in.—receding). The displacement

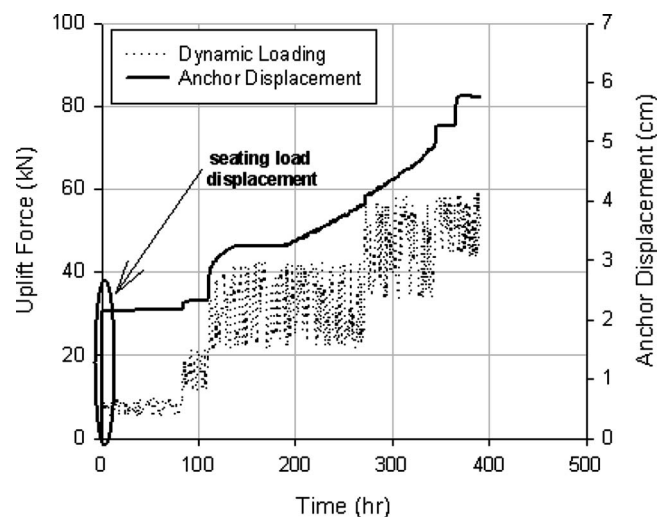


Fig. 8. Anchor V6 (2-helix) long-term dynamic test

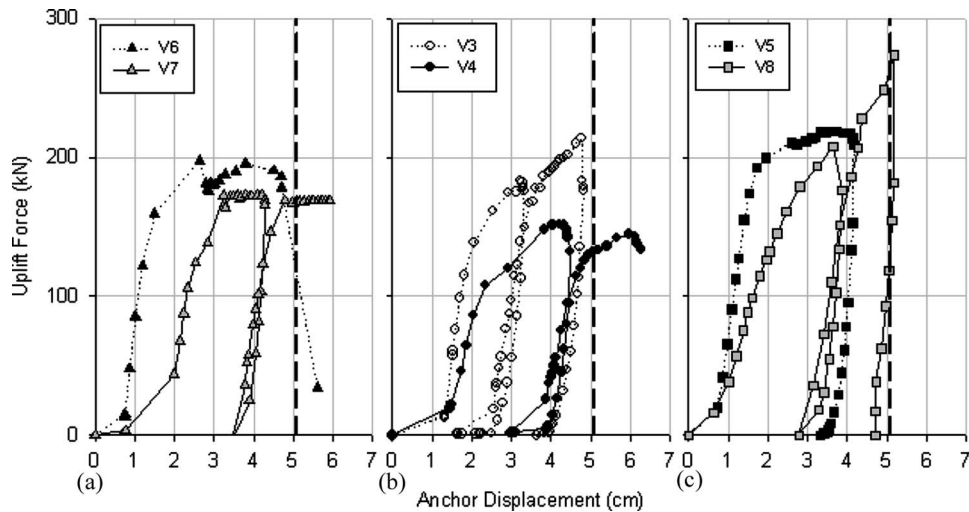


Fig. 9. Results of static uplift tests: (a) 2-helix; (b) 3-helix; and (c) 4-helix

rate and magnitude are very high in this 2-helix test (displacement scale on right side of figure doubles from 3.5 cm to 7 cm). As can be seen, when the dynamic loading was maintained between 19.6 and 39.2 kN, the anchor crept continually for about 100 hours, and then continued to pull-out as the load was increased. This shows that in a 80.5–96 km/h (50 to 60 mi/h) regime, in this particular soil type, using a 2-helix anchor would result in excessive creep.

Effects of Dynamic Loading on Uplift Capacity

Five anchors (V3, V4, V5, V6, and V8) were dynamically loaded for 2 to 4 weeks, followed by a postdynamic static test. V7 was only statically tested to have a comparison anchor to V6 to show the effects (if any) of dynamic loading on long-term uplift capacity. Fig. 9 presents the results of the static uplift tests delineated by geometry. A companion paper specifically discusses the influence of anchor geometry on the long-term performance of anchors under dynamic loading (Cerato and Victor 2008). A direct-performance comparison between each group was not possible due to the fact that there were several different variable conditions from test to test (e.g., variable subsurface properties, installation depths, installation torques, water table conditions, etc.). A trend that is noticeable in the data is that in general, higher loads were experienced with additional helical plates. Also, in the unload-reload cycles, it can be seen that the anchors never return to a zero displacement.

It can be seen that V6 slightly outperforms V7. V6 was dynamically loaded and then statically tested, while V7 was just statically tested. This increase in capacity may be an indicator that dynamically loading an anchor improves the long-term anchor uplift, but there are too many variables to conclude this observation. Both anchors had the same installation and testing water table depth and similar torque values up until 4.5 m, after which, V7 advances through a relatively weak layer from 5.2–7.1 m. Locating the top helix in the relatively soft sand may explain why V7 does not have as high of an uplift capacity.

In the 3-helix anchor tests (V3 and V4), V3 significantly outperforms V4. Both tests had similar water table conditions during installation and testing and similar torque installation profiles, with V4 having slightly higher values than V3. Therefore, these

anchors were thought to perform similarly. One noted difference that could affect the long-term uplift capacity, however, is that V3 was dynamically loaded under much higher loads than V4 (double to triple the loads). Since everything else about this test was similar (installation torque, depth and water table conditions), it can be seen that dynamically loading an anchor at relatively high cyclic loads/static uplift capacity ratios (0.25–0.40) may significantly increase uplift capacities. This high load ratio should also reduce creep, which can be seen to occur in these two tests. V4 was tested with ratios ranging from 0.15–0.25 and showed a lower uplift capacity and a higher rate of creep. This observation is helpful when designing a prestressing program for helical anchors for use as guyed cables. Both a magnitude, duration and load ratio are important to understand and implement into a field program to achieve the desired lifetime performance.

Both 4-helix anchors (V5 and V8) were dynamically loaded with the same magnitude and duration, and therefore had similar cyclic loads/static uplift capacity ratios (0.1–0.3). Anchor V5 had a much higher torque profile at a shallower depth than V8, which failed to reach the design torque even at 25 feet. The water table for Anchor V5 was at 2.5 m for the duration of the test and the water table rose from 3 m to 2.5 m throughout V8's test. It was thought that V5 would out-perform V8 because of the differences in torque installation values, however, both anchors performed similarly in uplift, with V8 showing a higher creep rate. This behavior may be explained because V8 is deeper ($H/D=12.9$) than V5 and located in a soft sand deposit, which may have been densified during the 600 h of cyclic loading. The anchor has much more soil bearing on the top helix, and therefore, shows a higher uplift capacity than predicted (predicted uplift/actual field capacity ratio=0.49), but creeps much more because of the disturbance during installation in a soft soil above and below all 4 helices. V5, on the other hand, is shallower ($H/D=6.9$) in a denser soil deposit, with less disturbance during installation, and therefore shows an uplift capacity much closer to the predicted value (predicted uplift/actual field capacity ratio=0.94).

Effects of Groundwater Variation on Static Uplift Capacities

The anchor comparison used to illustrate the effects that a varying water table from installation to testing can have on the uplift

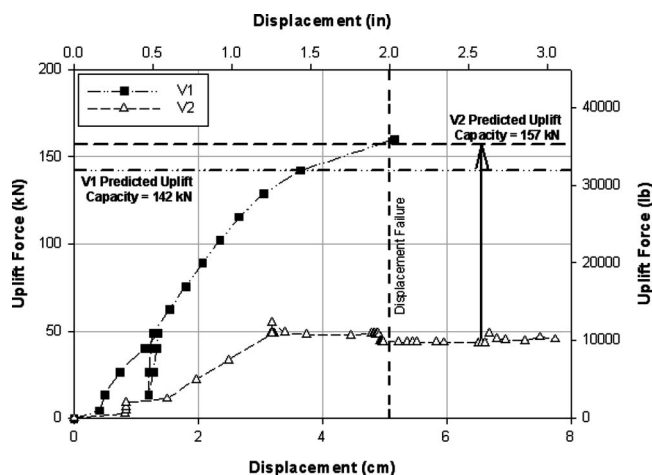


Fig. 10. Static uplift comparison of Anchors V1 and V2

capacity of helical anchors is between anchors V1 and V2. Referring back to Fig. 4 the installation torque of each anchor indicates that the anchors were supposed to perform similarly. Fig. 10 shows the difference in uplift performance of anchors V1 and V2 after effective stress conditions change from installation to testing. The water table rose about 1.46 m (4.83 ft) between installation and testing of Anchor V1, which did not submerge any of the 4 helices [bottom helix was at 3.0 m (10 ft)], and therefore, did not affect uplift capacity. The water table rose 2.8 m (9.08 ft) between installation and testing of Anchor V2, from 1.5 m (5 ft) below the bottom helix to directly above the top helix. Anchor V2 helices were totally submerged by the water table and the effective stress of the foundation soil decreased, therefore, decreasing the uplift capacity. If V2 was attached to a guyed cable and the water table rose to this extent, the foundation may have failed. Even though a more than adequate torque profile was recorded for this 2-helix anchor, a rising water table cut the capacity 3-fold. In this case, the predicted uplift capacity from the torque correlation method severely overpredicted the capacity due to not incorporating life-time environmental changes in the design. If additional site conditions had been known at the time of installation, the anchor would have been installed so that the top helix was below the lowest known water table to avoid loss of effective stress when the water table rose.

Comparison of Helical Anchor Prediction Methods

This investigation compared the helical anchor uplift capacity prediction results of analytical and torque correlation methods. The two analytical approaches chosen to predict uplift behavior were methods used by Rao et al. (1990); cylindrical shear and series plate method. The cylindrical failure surface model used by Rao et al. (1990) to analyze anchors in clay is as follows:

$$Q = c_u A_s' + \alpha c_u A_s \quad (2)$$

where A_s' = surface area of cylinder between top and bottom helical plates [m^2 (ft^2)]; A_s = surface area of pile shaft [m^2 (ft^2)]; c_u = in situ vane shear strength measured [kPa (lb/ft^2)]; and α = adhesion factor (dimensionless).

This cylindrical shear method was slightly modified to encompass the heterogeneous subsurface layered profile, where friction

angle properties were used in the sand layer and undrained shear strength properties in the clay layer. Due to the fact that the majority of the anchors were deep foundations and a significant amount of resistance came from bearing resistance on the top layer, the equation was also modified to include the bearing resistance on the top helix, similarly to how Mitsch and Clemence (1985) modeled the failure surface of deep multi-helix anchors. The bearing surface on the top helix was chosen with the requirement that a 1.21 m (4 ft) layer of the soil rest on the top helix to be used in the analysis as the overburden soil. Another modification to the equation was the exclusion of the shaft (adhesion) resistance, because observations during installation indicated that at some positions along the anchor shaft the soil was not in contact. The final equation followed as:

$$Q_u = f_s A_s' \text{ (friction)} + f_s F_c A \text{ (bearing)} \quad (3)$$

where $f_s = c_u$ —for clay/silt or $k\sigma' \tan\Phi'$ —for sand [kPa (lb/ft^2)]; σ' = effective stress [kPa (lb/ft^2)]; A = area of top helix [m^2 (ft^2)]; F_c = nondimensional uplift capacity factor; Φ' = effective friction angle ($^\circ$); and $k = 1 - \sin(\Phi')$ —at rest lateral coefficient.

The nondimensional uplift capacity factor used for analysis was taken from Das (1985) as $F_c = 9$ (for square and circular anchors). The undrained shear strength, rather than in situ vane shear strength, was estimated from a consolidated isotropic undrained compression (CIUC) tri-axial test as 58 kPa (1,210 lb/ft^2) for Layer 1, and SPT blow counts were used to estimate the cohesion in Layers 2 and 4 [c (ksf) = $N/8$]. The effective friction angle of 35° in Layer 3 was from a borehole shear test (BST). The diameter of the cylindrical surface was estimated as the diameter of the top helix of each anchor. The effective stresses were calculated at the mid-height of the cylinder.

The bearing plate model used by Rao et al. (1990) to analyze anchors in cohesive or cohesionless soil is as follows:

$$Q_u = A c N_c \text{ (cohesive)} \quad (4)$$

$$Q_u = A q' N_q = A \gamma' D N_q \text{ (cohesionless)} \quad (5)$$

where A = projected helix area [m^2 (ft^2)]; c = cohesion [kPa (lb/ft^2)]; N_c = bearing capacity factor for cohesive component of soil = 9; γ' = effective unit weight of the soil [kN/m^3 (pcf)]; D = vertical depth to helix plate [m (ft)]; and N_q = bearing capacity factor for noncohesive component of soil.

Provided that the helix spacing on the helical anchor is greater than, or equal to 3 helix diameters, the capacity of the individual helices on a multi-helix anchor can be summed to obtain the total ultimate capacity of a specific helical anchor. The depth term for each additional helix beneath the top helix for multi-helix anchors is calculated as 3 helix diameters above the helix plate.

The torque correlation model used was proposed by Hoyt and Clemence (1989), which uses a torque correlation factor, K_t , to predict the uplift capacity. An industry recommended default factor of $33 m^{-1}$ ($10 ft^{-1}$) was used in the analysis. Average torques of the last 1 m (3 ft) measurements were used instead of the final torques to calculate uplift capacity. Table 3 summarizes the geometry, water table conditions at installation and testing, the field results and the predictions of the cylindrical failure surface, bearing plate and torque correlation method. The agreement ratio in the table is the ratio of the predicted value over the actual value of the uplift capacity. An agreement ratio under 1 signifies that the capacity was underpredicted and vice versa for values over 1. The closer the agreement ratio to 1, unity, the better the prediction method was for that condition.

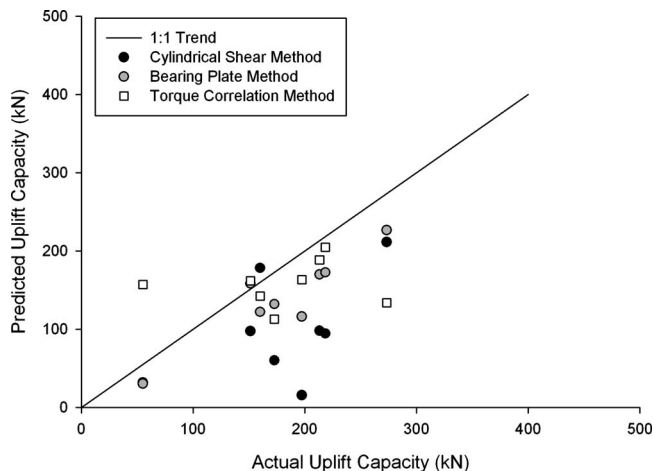
Table 3. Summary of Helical Anchor Performance

Anchor symbol	Number of helix	Water table install/testing (m)	Average final torque [kN-m (lb-ft)]	Field test static uplift capacity [kN (lb)]	Torque correlation predicted ultimate uplift capacity [kN (lb)]	Cylindrical shear method predicted ultimate uplift capacity [kN (lb)]	Bearing plate method predicted ultimate uplift capacity [kN (lb)]
V1	4	4.57/3.1	4.6 (3,200)	159.9 (35,950)	142.0 (31,922)	177.8 (39,970)	122 (27,775)
V2	2	4.57/1.8	5.3 (3,500)	55.1 (12,380)	157.0 (35,295)	31.6 (7,100)	30.6 (6,890)
V3 ^a	3	1.95/3.2	4.0 (2,970)	212.9 (47,865)	188.1 (42,273)	97.8 (21,985)	171 (38,450)
V4 ^a	3	1.95/3.1	4.9 (3,633)	151.2 (33,990)	235.5 (52,931)	97.2 (21,850)	159 (35,830)
V5 ^a	4	1.95/3.1	6.2 (4,600)	218.3 (49,060)	204.4 (45,940)	94.1 (21,144)	174 (39,067)
V6 ^a	2	1.95/2.8	5.0 (3,666)	197.2 (44,300)	162.9 (36,623)	15.5 (3,479)	116 (26,277)
V7	2	1.95/2.8	2.4 (1,766)	172.6 (38,800)	112.5 (25,295)	60.0 (13,485)	133 (29,881)
V8 ^a	4	1.95/2.6	4.1 (3,000)	273.1 (61,380)	133.3 (29,960)	211.1 (47,445)	228 (51,309)

Note: Bold data are anchors that did not meet design average final torques.

^aDynamically tested.

Fig. 11 gives a comparison plot of the three methods (torque correlation, cylindrical shear, and bearing plate) to a 1:1 line (100% agreement between predicted and actual values). Any data point below the 1:1 line was an underprediction by the method and any point above the line was an overprediction. The data shows that each method generally underpredicted the capacities of all anchors. The larger agreement ratio (overpredictions) using the torque correlation method was due to rising water table after installation (V2). 2-helix anchor capacity was significantly underpredicted by the analytical approach primarily due to the fact that the cylindrical failure surfaces are much smaller in 2-helix geometries. Another factor that may affect the cylindrical shear underpredictions may be the inability to incorporate the different overburden pressures or overconsolidation conditions that exist on a top helix. The bearing plate method predicted the uplift capacity better than the cylindrical shear method and was comparable to the torque correlation for six anchors. In four of five post-dynamic static anchor tests, both prediction methods underpredicted the uplift capacities. The performance of the anchors in actual uplift may have been enhanced by the dynamic loading densifying the soil, therefore, resulting in higher uplift capacities than were predicted.

**Fig. 11.** Uplift performance prediction plot

Conclusions

An extensive field testing program was devised to investigate uplift prediction methods used in helical anchor design as well as the effects of long-term dynamic loading and fluctuating water table on helical anchor performance subjected to long-term dynamic loading for 1–10 kW wind tower guyed cable foundations. A preexisting well was used to monitor water table levels over the course of the testing program. From the results of this field case study, it was found that:

- Dynamically loading an anchor at relatively high cyclic loads/static uplift capacity ratios (0.25–0.40) may significantly increase uplift capacities and minimize long-term creep. A dynamic, anchor pre-loading program should be implemented to properly seat the anchors to achieve the desired lifetime performance. Without a preloading program, the anchors could move excessively under relatively low loads, causing tower stability problems. The magnitude, duration and load ratio is important to understand and implement into a field program to achieve the desired lifetime performance.
- Water table fluctuations after installation can significantly affect short- and long-term uplift capacity. A rise of 3.9 m (13 ft) in water table from below to above all helices lowered the predicted anchor capacity 3-fold. Therefore, it is recommended that all anchors be installed so that the top helix is below the lowest known water table to avoid losing strength when the water table rises. Uplift capacity will only increase if the water table recedes below the anchor.
- The cylindrical shear prediction method was found to significantly underpredict actual uplift capacities of 7 of 8 anchors tested. This method relies heavily on accurate soil test data (lab and in situ) from the same soil layers that the helices are in, under the same environmental conditions. The subsurface variability, sampling and testing limitations, in terms of time and money, as well as changing conditions (e.g., water table levels) make this method very difficult to accurately employ. The cylindrical shear equation cannot incorporate the different overburden pressures or overconsolidation conditions that exist on a top helix, which may be a reason for the significant underprediction.
- The bearing plate analytical uplift capacity prediction method was found to be a better predictor than the cylindrical shear method, and comparable to the torque correlation method in six of the anchors, however, still generally underpredicted the

uplift capacity of the anchors. This underprediction could be partially because the dynamic testing densified the soil and increased the actual static uplift capacity of the anchor.

- The torque correlation method underpredicted 6 of 8 anchors tested, possibly due to the strengthening effects that dynamic loading had on the static uplift capacity. The torque correlation method overpredicted one anchor capacity because of the water table rising above the anchor's top helix from installation to testing. If the anchor is placed well below a fluctuating water table the torque correlation method seems to predict capacities better than the analytical approach.

Acknowledgments

This research project was funded by the Oklahoma Center for the Advancement of Science and Technology (OCAST), Project No. AR062.007, and is a joint venture with Bergey Windpower Company, Inc. The writers are grateful for the time, support, and material donations from Hubbell Power Systems/Chance Civil Construction. We would also like to thank our installers from Atlas Systems of Oklahoma, Sam Lowry and Mike Schweighardt; and Michael Schmitz, Fears Structural Lab Supervisor; and Russell Buhler, Geotechnical Engineering Undergraduate Researcher, for their technical assistance with this project.

References

- Andreadis, A., Harvey, R. C., and Burley, E. (1981). "Embedded anchor response to uplift loading." *J. Geotech. Engrg. Div.*, 107(GT1), 59–78.
- Cerato, A. B., and Victor, R. (2008). "Effects of helical anchor geometry on long-term performance for small wind tower foundations subject to dynamic loads." *J. Deep Foundations Inst. (DFI)*, 2, 30–41.
- Clemence, S. P., and Smithling, A. P. (1984). "Dynamic uplift capacity of helical anchors in sand." *Proc., 4th Australia-New Zealand Conf., Geomechanics*, 1, 88–93.
- Das, B. M. (1985). "Resistance of shallow inclined anchors in clay." *Uplift behavior of anchor foundations in soil*, S. P. Clemence, ed., ASCE, New York, 86–101.
- Dejong, J. T., Randolph, M. F., and White, D. J. (2003). "Interface load transfer degradation during cyclic loading a microscale investigation." *Soils Found.*, 43(4), 81–93.
- Dejong, J. T., White, D. J., and Randolph, M. F. (2006). "Microscale observation and modeling of soil-structure interface behaviour using particle image velocimetry." *Soils Found.*, 46(1), 15–28.
- Ghaly, A. M., and Clemence, S. P. (1999). "Closure to pullout performance of inclined helical screw anchors in sand." *J. Geotech. Geoenviron. Eng.*, 125(12), 1102–1104.
- Hanna, T. H., and Mosawe, M. J. (1981). "Performance of prestressed anchors under slow repeated loadings." *Proc., 10th Int. Conf. on Soil Mechanics and Foundation Engineering*, Stockholm, Sweden, Vol. 2, 127–133.
- Hanna, T. H., Sivapalan, E., and Senturk, A. (1978). "The behaviour of dead anchors subjected to repeated and alternating loads." *Ground Eng.*, 2(4), 28–34.
- Hargrave, R. L., and Thorsten, R. E. (1992). "Helical piers in expansive soils of Dallas, Texas." *Proc., 7th Int. Conf. on Expansive Soils*, 1, 125–130.
- Hovland, H. J. (1993). "Discussion of 'Helical anchors in dry and submerged sand subjected to surcharge.'" *J. Geotech. Engrg.*, 119(2), 391–392.
- Hoyt, R. M., and Clemence, S. P. (1989). "Uplift capacity of helical anchors in soil." *Proc., 12th Int. Conf. on Soil Mechanics and Foundation Engineering*, Vol. 2, 1019–1022.
- Mitsch, M. P., and Clemence, S. P. (1985). "The uplift capacity of helix anchors and sand." *Uplift behavior of anchor foundations in soil*, ASCE, New York, 26–47.
- Mooney, J. S., Adamczak, S., Jr., and Clemence, S. P. (1985). "Uplift capacity of helix anchors in clay and silt." *Uplift behavior of anchor foundations in soil*, ASCE, New York, 48–72.
- Pack, J. S. (2000). "Design of helical piles for heavily loaded structures." *New technological and design developments in deep foundations*, ASCE, 353–367.
- Perko, H. A. (2000). "Energy method for predicting the installation torque of helical foundations and anchors." *New technological and design developments in deep foundations*, ASCE, 342–352.
- Prasad, Y. V. S. N., and Rao, S. (1994). "Pullout behavior of model piles and helical pile anchors subjected to lateral cyclic loading." *Can. Geotech. J.*, 31(1), 110–119.
- Rao, S., Prasad, Y. V. S. N., and Prasad, C. V. (1990). "Experimental studies on model screw pile anchors." *Proc., Indian Geotechnical Conf.*, Vol. 1, 465–468.
- Trofimenkov, J. G., and Maruipolshii, L. G. (1965). "Screw piles used for mast and tower foundations." *Proc., 6th Int. Conf. on Soil Mechanics and Foundation Engineering*, Vol. 2, 328–332.